Pis'ma v ZhETF, vol. 101, iss. 7, pp. 534 – 541 April 10

Controlling of Goos-Hänchen shift via biexciton coherence in a quantum dot

S. H. Asadpour[1)], *R. Nasehi*[+], *M. Mahmoudi*[+], *H. R. Soleimani*

Department of Physics, University of Guilan, P. O. Box 1914, 41335 Rasht, Iran

[+]*Department of Physics, Zanjan University, P. O. Box 45195-313, Zanjan, Iran*

Submitted 14 January 2015
Resubmitted 2 March 2015

Controlling of the Goos–Hönchen (GH) shifts of the reflected and transmitted probe pulses through a cavity containing four-level GaAs/AlGaAs quantum dot with 15 periods of 17.5 nm GaAs wells and 25-nm $Al_{0.3}Ga_{0.7}As$ barriers is investigated. Under appropriate conditions, the probe absorption can be converted to the probe gain, therefore the controlling of negative and positive GH shift in the both reflected and transmitted probe beams can be occurred simultaneously. Our obtained results show that the group index of the probe beams could be negative or positive in both reflected and transmitted pulses. Therefore, simultaneous subluminal or superluminal light propagation in reflected and transmitted pulses can be achieved.

DOI: 10.7868/S0370274X15070127

Introduction. It is known that in geometrical optics, reflected and transmitted light beams can be laterally shifted from the position. This, firstly observed experimentally by Goos and Hänchen (GH shifts) [1], in 1947. The lateral shifts happen between the totally reflected light beam and the incident light beam when a total reflection happens at the interface of two medium [2]. There are some interesting applications in GH shifts for optical sensing and measurements [3], which can measure various quantities such as beam angle, refractive index and displacement. Moreover, in negative refractive index waveguide as compared with the regular dielectric waveguide due to the negative GH shifts, the amplitude of electric field can be greatly enhanced [4]. The GH shift also can be used as a characterization of the permeability μ and permittivity ε of the materials [5] and in the design of surface Plasmon resonance waveguide device at range μm [6]. Therefore, it is worth studying the control and manipulation of GH shifts in a fixed configuration. For explain the positive and negative GH shift various theoretical and experimental schemes have been proposed. For example, Merano et al. [7] studied the Goos–Hänchen effect experimentally for the case of an optical beam reflecting from a metal surface (gold) at 826 nm. They reported a negative lateral shift of the reflected beam in the plane of the incident beam for a *p*-polarization and a positive shift for the *s*-polarization case. Recently, investigating of the GH shifts in a slab system or left-handed materials has been done. Berman [8] and Lakhtakia [9] studied the negative GH shifts at an interface between "normal" and left-handed media. Kong et al. [10] elaborated the lateral displacement of a Gaussian-shaped beam reflected from a grounded slab with simultaneously negative permittivity and permeability. It is also found that GH shifts of the transmitted beam through a slab of left-handed medium can be negative as well as positive [11].

It is known that the quantum coherence and interference has an essential role for controlling the absorption and dispersion properties of an atomic medium. This control over the dispersive properties of the atomic systems can lead to an electromagnetically induced transparency (EIT) [12], optical solitons [13, 14], optical bistability [15, 16], electron localization [17, 18], and other phenomenon [19–21]. Based on this fact, some models have been proposed for controlling of the GH shifts by using two, three and four-level atomic systems inside a cavity [22, 23]. Therefore, by using quantum coherence and interference, controlling of GH shift can be done without changing the structure of the fixed device or atomic configuration [22, 23] inside the cavity. In these configurations it is shown that the GH shifts can be controlled by manipulation of the dispersive properties of the intracavity. In a recent work by Ziauddin and Qamar [24], they proposed a Gain-assisted model for controlling the GH shifts in a cavity containing three-level dilute gaseous atomic medium. They found that by manipulation of the detuning associated with the probe light field which interacts with the intracavity medium during its propagation through the cavity can lead to

[1)]e-mail: S.Hosein.Asadpour@gmail.com

a control over negative and positive GH shift in the reflected and transmitted light beam via the anomalous and normal dispersion of the medium.

Recently, many kinds of phenomena based on the quantum interference and coherence have also been extensively studied in the semiconductors quantum wells (SQW). For the intersubband transitions in SQW, we can say that it behaves as an artificial atom [25]. Therefore many interesting phenomena based on quantum coherence and interference in SQWs has been discussed, such as optical bistability [26–30], four-wave mixing [31–33], Kerr nonlinearity [34, 35], and others [36–48]. The devices based on intersubband transitions in the SQW have many inherent advantages such as the large electric dipole moments due to the small effective electron mass, the great flexibilities in devices design by choosing the materials and structure dimensions, the high nonlinear optical coefficients. The majority of the theoretical analyses of the above works in SMQWs are based on atomic quantum coherence theory [49]. A complete description of many-body effect such as Coulomb interaction between charged carriers has not been considered. It is known that in direct-gap semiconductors, excitons play an essential role in optical processes near the fundamental band edge. It has been shown that excitonic non-radiative coherence, including exciton spin coherence and biexciton coherence, can lead to EIT processes in quantum wells [36–38]. By predominant the rapid decoherence with ultra fast laser pulses and by using and restrains the many-body Coulomb interactions, the realization of the excitonic EIT processes in QWs has been made possible. With intersubband coherence between different conduction subbands [39–41] and different valance subbands [42], and with intervalence band coherence between the heavy-hole (HH) and light-hole (LH) valance bands [43, 44], EIT processes have also been observed. Various EIT processes have also been explored experimentally [45] as well as theoretically in QDs [46–48].

Recently, the Goos–Hänchen effect and Fano resonance have been studied in photonic crystals that are considered Fourier counterparts in wave-vector-coordinate space. The Goos–Hänchen effect, which was enhanced by the excitation of Bloch surface electromagnetic waves, was visualized using far-field microscopy and measured at the surface of photonic crystals by angular spectroscopy. The maximal Goos–Hänchen shift was observed to be 66 μm [50].

In this paper, we propose a new model for controlling the GH shifts behavior based biexciton coherence in a quantum dot nanostructure. Recently, we analyzed optical bistability and multistability based biexciton coherence in a multiple quantum well nanostructure [51]. We showed that biexciton energy renormalization which resulted from biexciton coherence can change the intensity threshold of optical bistability and multistability. In another study, phase control of optical bistability and multistability based biexciton coherence were also discussed [52]. Following the similar scheme, we here study the behavior of the GH shifts for the corresponding superluminal and also for the subluminal propagation of the light through the intracavity medium. Here, a four-level GaAs/AlGaAs as semiconductor structure with 15 periods of 17.5 nm GaAs layer and 25-nm $Al_{0.3}Ga_{0.7}As$ barriers is used as an intracavity. It is found that biexciton coherence and relative phase of applied fields has a major role on controlling GH shifts of probe beams reflected from or transmitted through a cavity.

Model and equation. Three layers with a structure ABA can be considered as a model of cavity. Two side layers A, with the same thickness $d_{\rm A}$ and permittivity $\varepsilon_{\rm A}$ are nonmagnetic dielectric slabs and are considered as walls of the cavity. Layer B is the intracavity medium with thickness $d_{\rm B}$ and permittivity $\varepsilon_{\rm B}$ (Fig. 1). The gas atoms [27] or semiconductor layer [48] can be used as an intracavity medium. The intracavity medium consists of four-level biexciton-exciton cascade scheme of GaAs/AlGaAs quantum dot with 15 periods of 17.5 nm GaAs wells and 25-nm $Al_{0.3}Ga_{0.7}As$ barriers. A TE-polarized light beam with angular frequency ω is incident on one side of the cavity which is in the vacuum with permittivity $\varepsilon_0 = 1$. The incident pulse makes an angle θ with the z-axis. This field is either reflected back or transmitted through the cavity with a lateral shifts (GH shifts). Generally, the electric and magnetic fields at two positions z and $z + \Delta z$ in the $j^{\rm th}$ layer can be related to each other via a transfer matrix as:

$$M_j(k_y, \omega, d_j) = \begin{pmatrix} \cos[k_z^j d_j] & \dfrac{i \sin[k_z^j d_j]}{q_j} \\ \dfrac{i \sin[k_z^j d_j]}{q_j} & \cos[k_z^j d_j] \end{pmatrix}, \quad (1)$$

where $k_z^j = \sqrt{\varepsilon_j k^2 - k_y^2}$ is the z component of the wave vector in $j^{\rm th}$ layer, k_y is the y component of wave vector in vacuum $k = \omega/c$. Here, c is the speed of light in vacuum, and parameter q_j is defined as $q_j = k_z^j/k$. d_j is the thickness, and j represents the $j^{\rm th}$ layer of the medium. Since the cavity has three layers, the total transfer matrix of the cavity is given by:

$$\mathrm{X}(k_y, \omega) = M_{\rm A}(k_y, \omega, d_{\rm A}) M_{\rm B}(k_y, \omega, d_{\rm B}) M_{\rm A}(k_y, \omega, d_{\rm A}), \quad (2)$$

where, $\mathrm{X}(k_y, \omega)$ represents the total transfer matrix connecting the fields at incident end and at the exit end.

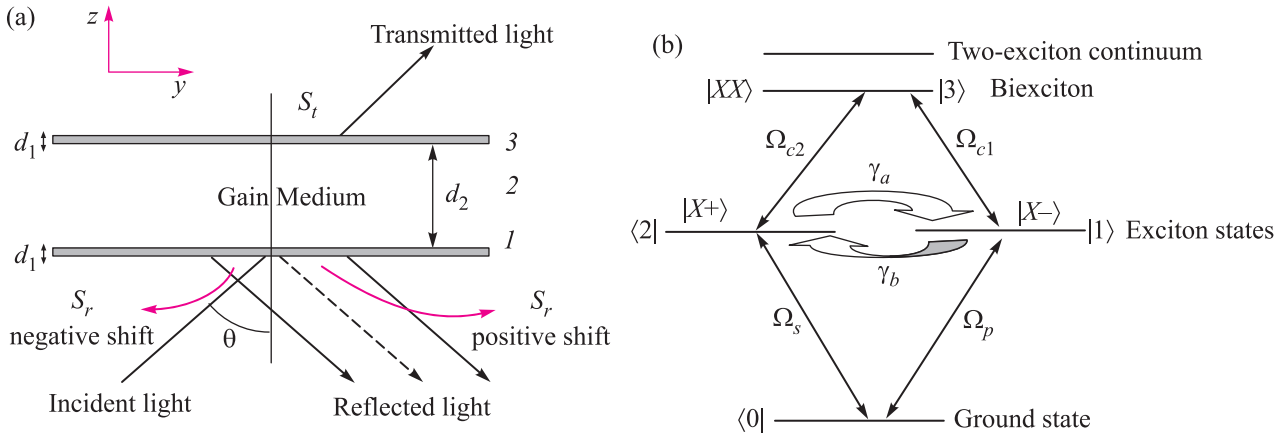

Fig. 1. (a) (color online) – Schematic diagram of the GH shifts of the reflected and transmitted light beams in a fixed cavity. The cavity contains a four-level GaAs/AlGaAs quantum dot with 15 periods of 17.5 nm GaAs wells and 25-nm $Al_{0.3}Ga_{0.7}As$ barriers. S_r, S_t are the reflected and transmitted beams of the GH shifts, respectively. The red arrows displays the incident probe beam, while the green and blue arrows shows the two coupling fields. (b) – Energy levels and transitions of the exciton-biexciton states. $|0\rangle$ – ground state, $|1\rangle$ and $|2\rangle$ – one-exciton states, $|3\rangle$ – biexciton state (or two-exciton continuum state). The medium interacts with two laser control fields and two pulsed probe and signal fields

From the transfer matrix method, the transmission coefficient $t(k_y,\omega)$ and the reflection coefficient $r(k_y,\omega)$ can be given as:

$$t(k_y,\omega)=\frac{2q_0}{[q_0(X_{22}+X_{11})]-[q_0^2X_{12}+X_{21}]}, \qquad (3)$$

$$r(k_y,\omega)=\frac{[q_0(X_{22}-X_{11})]-[q_0^2X_{12}-X_{21}]}{[q_0(X_{22}+X_{11})]-[q_0^2X_{12}-X_{21}]}, \qquad (4)$$

where $q_0=\sqrt{\varepsilon_0-\sin^2\theta}$. Parameter $X_{ij}(k_y,\omega_p)$ $(i,j=1,2)$ is the element of matrix $\mathrm{X}(k_y,\omega)$. It can be seen that the transmission and reflection coefficients depend on the permittivity and thickness of the cavity walls, permittivity and thickness of the intracavity medium, and the incident angle of the probe field. The permittivity of intracavity medium ε_{B} can be related to the susceptibility of the four-level quantum dot via

$$\varepsilon_{\mathrm{B}}=1+\chi(\omega), \qquad (5)$$

where $\chi(\omega)=\chi'(\omega)+\chi''(\omega)$, $\chi'(\omega)$, $\chi''(\omega)$ are the real and imaginary parts of $\chi(\omega)$, which represent the dispersion and the absorption properties of the intracavity medium, respectively. By using the stationary phase theory, the lateral shift in the reflected and transmitted light beams can be given as:

$$S_{r,t}=-\frac{\lambda}{2\pi}\frac{d\varphi_{r,t}}{d\theta}, \qquad (6)$$

where $\varphi_{r,t}$ are the phases associated with the reflection $r(k_y,\omega)$ and transmission $t(k_y,\omega)$ coefficients. Thus, the lateral shifts of the transmitted and reflected probe light beams can be expressed as:

$$S_t=-\frac{\lambda}{2\pi}\frac{1}{|t(k_y,\omega)|^2}\left\{\mathrm{Re}[t(k_y,\omega)]\frac{d(\mathrm{Im}[t(k_y,\omega)]}{d\theta}-\right.$$
$$\left.-\mathrm{Im}[t(k_y,\omega)]\frac{d(\mathrm{Re}[t(k_y,\omega)]}{d\theta}\right\}, \qquad (7)$$

$$S_r=-\frac{\lambda}{2\pi}\frac{1}{|r(k_y,\omega)|^2}\left\{\mathrm{Re}[r(k_y,\omega)]\frac{d(\mathrm{Im}[r(k_y,\omega)]}{d\theta}-\right.$$
$$\left.-\mathrm{Im}[r(k_y,\omega)]\frac{d(\mathrm{Re}[r(k_y,\omega)]}{d\theta}\right\}. \qquad (8)$$

We now discuss the level structure of the doped four-level GaAs/AlGaAs quantum dot nanostructure with 15 periods of 17.5 nm GaAs layer and 25-nm $Al_{0.3}Ga_{0.7}As$ barriers as a dispersive layer of slab. This system is same as one employed in Ref. [53]. As shown in Fig. 1, the ground state $|0\rangle$, one-exciton states $|1\rangle$, $|2\rangle$, and biexciton state $|3\rangle$, resemble a four-level double cascade configuration. In the present system, two probe fields with angular frequencies $\omega=\omega_{p,s}$, one-half Rabi frequencies $\Omega_{p,s}$, and two continues wave coherent couple fields with angular frequency $\omega_{c1(c2)}$, one-half Rabi frequency $\Omega_{c1(c2)}$, complete the respective excitations. In this system, the exciton coherence is the nonradiative coherence, which can lead to destructive interference in the optical transition between the one-exciton and bound biexciton states. Under the rotating wave approximation and electric dipole approximations and including to the free energy term, the total Hamiltonian can be written as:

$$H=H_0+H_{\mathrm{int}}^I, \qquad (9)$$

$$H_0 = \hbar\omega_0|0\rangle\langle 0| + \hbar\omega_1|1\rangle\langle 1| + \hbar\omega_2|2\rangle\langle 2| + \hbar\omega_3|3\rangle\langle 3|, \quad (10)$$

$$H_{\text{int}}^I = \Omega_p e^{-i\omega_p t} e^{i\varphi_p}|1\rangle\langle 0| + \Omega_s e^{-i\omega_s t} e^{i\varphi_s}|2\rangle\langle 0| + \\ + \Omega_{c1} e^{-i\omega_{c1} t} e^{i\varphi_{c1}}|3\rangle\langle 1| + \Omega_{c2} e^{-i\omega_{c2} t} e^{i\varphi_{c2}}|3\rangle\langle 2|. \quad (11)$$

The time evolution of the system, expressed using the density operator ρ, is governed by the Liouville equation which leads to the following equations for the density matrix elements ρ_{ij}:

$$\begin{aligned}
\dot\rho_{11} &= i\Omega_p(\rho_{01} - \rho_{10}) + i\Omega_{c1}(\rho_{31} - \rho_{13}) + \\
&+ \gamma_a\rho_{22} - (\gamma_b + \gamma_4)\rho_{11} + \gamma_2\rho_{33}, \\
\dot\rho_{22} &= i\Omega_s(\rho_{02} - \rho_{20}) + i\Omega_{c2}(e^{i\phi}\rho_{32} - e^{-i\phi}\rho_{23}) + \\
&+ \gamma_1\rho_{33} - (\gamma_3 + \gamma_a)\rho_{22} + \gamma_b\rho_{11}, \\
\dot\rho_{33} &= +i\Omega_{c2}(e^{-i\phi}\rho_{23} - e^{i\phi}\rho_{32}) + \\
&+ i\Omega_{c1}(\rho_{13} - \rho_{31}) - (\gamma_1 + \gamma_2)\rho_{33}, \\
\dot\rho_{10} &= -[1/2(\gamma_4 + \gamma_b + \gamma_{10}^{\text{dph}}) - i\Delta_1]\rho_{10} + \\
&+ i\Omega_p(\rho_{00} - \rho_{11}) + i\Omega_{c1}\rho_{30} - i\Omega_s\rho_{12}, \\
\dot\rho_{20} &= -[1/2(\gamma_3 + \gamma_a + \gamma_{20}^{\text{dph}}) - i\Delta_2]\rho_{20} + \\
&+ i\Omega_s(\rho_{00} - \rho_{22}) + i\Omega_{c2}e^{i\phi}\rho_{30} - i\Omega_p\rho_{21}, \\
\dot\rho_{30} &= -[1/2(\gamma_1 + \gamma_2 + \gamma_{30}^{\text{dph}}) - i\Delta_3]\rho_{30} + \\
&+ i\Omega_{c1}\rho_{10} + i\Omega_{c2}e^{-i\phi}\rho_{20} - i\Omega_s\rho_{32} - i\Omega_p\rho_{31}, \\
\dot\rho_{32} &= -[1/2(\gamma_1 + \gamma_2 + \gamma_3 + \gamma_{32}^{\text{dph}}) - i(\Delta_3 - \Delta_1)]\rho_{32} - \\
&- i\Omega_{c2}e^{i\phi}(\rho_{33} - \rho_{22}) - i\Omega_{c1}\rho_{21} + i\Omega_s\rho_{03}, \\
\dot\rho_{21} &= -[1/2(\gamma_b + \gamma_3 + \gamma_4 + \gamma_a + \gamma_{21}^{\text{dph}}) - i(\Delta_1 - \Delta_2)]\rho_{21} - \\
&- i\Omega_p\rho_{20} - i\Omega_{c1}\rho_{23} + i\Omega_{c2}e^{i\phi}\rho_{31} + i\Omega_s\rho_{01}, \\
\dot\rho_{31} &= -[1/2(\gamma_1 + \gamma_2 + \gamma_4 + \gamma_b + \gamma_{31}^{\text{dph}}) - i(\Delta_1 - \Delta_3)]\rho_{31} + \\
&+ i\Omega_p\rho_{03} + i\Omega_{c1}(\rho_{33} - \rho_{11}) - i\Omega_{c2}e^{i\phi}\rho_{12},
\end{aligned} \quad (12)$$

where $\rho_{ij} = \rho_{ij}^*$, $\Delta_j = \omega_{p(s)} - (\omega_j - \omega_0)$ $(j = 1, 2)$, $\Delta_3 = \omega_{p(s)} + \omega_{cj} - (\omega_3 - \omega_0)$. The former γ_j $(j = 1, 2, 3, 4)$ denotes the total decay rate of exciton and biexciton coherence, which are added phenomenologically in the above density matrix equations (12). The letter γ_{ij}^{dph} is the dephasing broadening linewidth, which may originate from electron-electron scattering, electron-phonon scattering, as well as inhomogeneous broadening due to scattering on interface roughness. Generally, γ_{ij}^{dph} is the dominant mechanism in a semiconductor solid-state system in contrast to the atomic systems. Here, γ_a, γ_b is decoherence rate of the exciton spin relaxation between the two exciton states respectively, and describes the spin decoherence between these states. And we have introduced $\phi = \varphi_s + \varphi_{c2} - \varphi_p - \varphi_{c1}$ as the relative phase of laser fields. In order to derive the linear susceptibility it is needed to obtain the steady state solution of density matrix equations. The density matrix elements can be expanded as $\rho_{ij} = \rho_{ij}^{(0)} + \rho_{ij}^{(1)} + \rho_{ij}^{(2)} + \ldots$. The zero$^{\text{th}}$ order solution of ρ_{00} will be identical, i.e., $\rho_{00}^{(0)} = 1$, and other elements are set to be zero. The matrix elements ρ_{10} and ρ_{20} are obtained as follows:

$$\rho_{10}^{(1)} = -\frac{(\Omega_{c2}^2 - d_2d_3)\Omega_p - \Omega_s\Omega_{c1}\Omega_{c2}e^{-i\phi}}{-d_1d_2d_3 + d_2\Omega_{c1}^2 + d_1\Omega_{c2}^2}, \quad (13)$$

$$\rho_{20}^{(1)} = \frac{(\Omega_{c1}^2 - d_1d_3)\Omega_s - \Omega_p\Omega_{c1}\Omega_{c2}e^{-i\phi}}{-d_1d_2d_3 + d_2\Omega_{c1}^2 + d_1\Omega_{c2}^2}. \quad (14)$$

And, $d_1 = i/2(\gamma_4 + \gamma_b + \gamma_{10}^{\text{dph}}) + \Delta_1$, $d_2 = [i/2(\gamma_3 + \gamma_a + \gamma_{20}^{\text{dph}}) + \Delta_2]$, $d_3 = [i/2(\gamma_1 + \gamma_2 + \gamma_{30}^{\text{dph}})] + \Delta_3$, first order susceptibilities of the two probe fields of the medium can be determined as:

$$\chi_p^{(1)} = \frac{N|\mu_{01}|^2}{2\hbar\varepsilon_0\Omega_p}(\rho_{10}^{(1)} + \rho_{20}^{(1)}). \quad (15)$$

Results and discussion. The GH shifts in the reflected and transmitted probe light beam under appropriate condition is discussed as follow. In the other words, we consider a TE-polarized light beam which incident by angle θ on the cavity is a probe light beam with frequency $\omega = \omega_{p(s)}$. At temperature up to 10 K, we select the real system parameters as $\gamma_1 = \gamma_2 = \gamma = 0.054$ meV and $\gamma_3 = \gamma_4 = 0.108$ meV , $\gamma_i^{\text{dph}} = 50$ meV, $\Delta_1 = \Delta_2 = \Delta_3 = 0$ [54] (which can be translated into the ratio with γ). Similarly in the following numerical calculations, all the parameters used are scaled by γ, which should be of the order of meV for the quantum well. The dependence of the GH shits of the reflected and transmitted probe beams versus incident angle for resonance condition of probe lights with different relative phase are displayed in Fig. 2. It can be seen that the GH shifts for the reflected and transmitted probe beams alter by changing the relative phase ϕ. In the other word, for $\phi = 0$ and $\phi = 2n\pi$, the GH shifts of reflected and transmitted probe beams are enhanced and have maximum values. Physically, at $\phi = 2n\pi$ the absorption of medium is very weak and near to zero, and medium is transparent for the applied probe lights. However, at $\phi = (2n+1)\pi/2$ and $(2n+1)\pi$, there exists strong absorption of the probe light beams when the probe beam is in resonance with atomic transition. Infact, the changing in linear susceptibility of the system by relative phase of applied fields makes the changing in the GH shifts of reflected and transmitted probe beams. The effect of relative phase on GH shifts of reflected and transmitted probe beams versus incident angle and for nonresonance condition of probe lights are shown in Fig. 3. For the case of $\phi = 0$, it is found that the similar behaviors with part a of Fig. 2 are obtained. Infact for

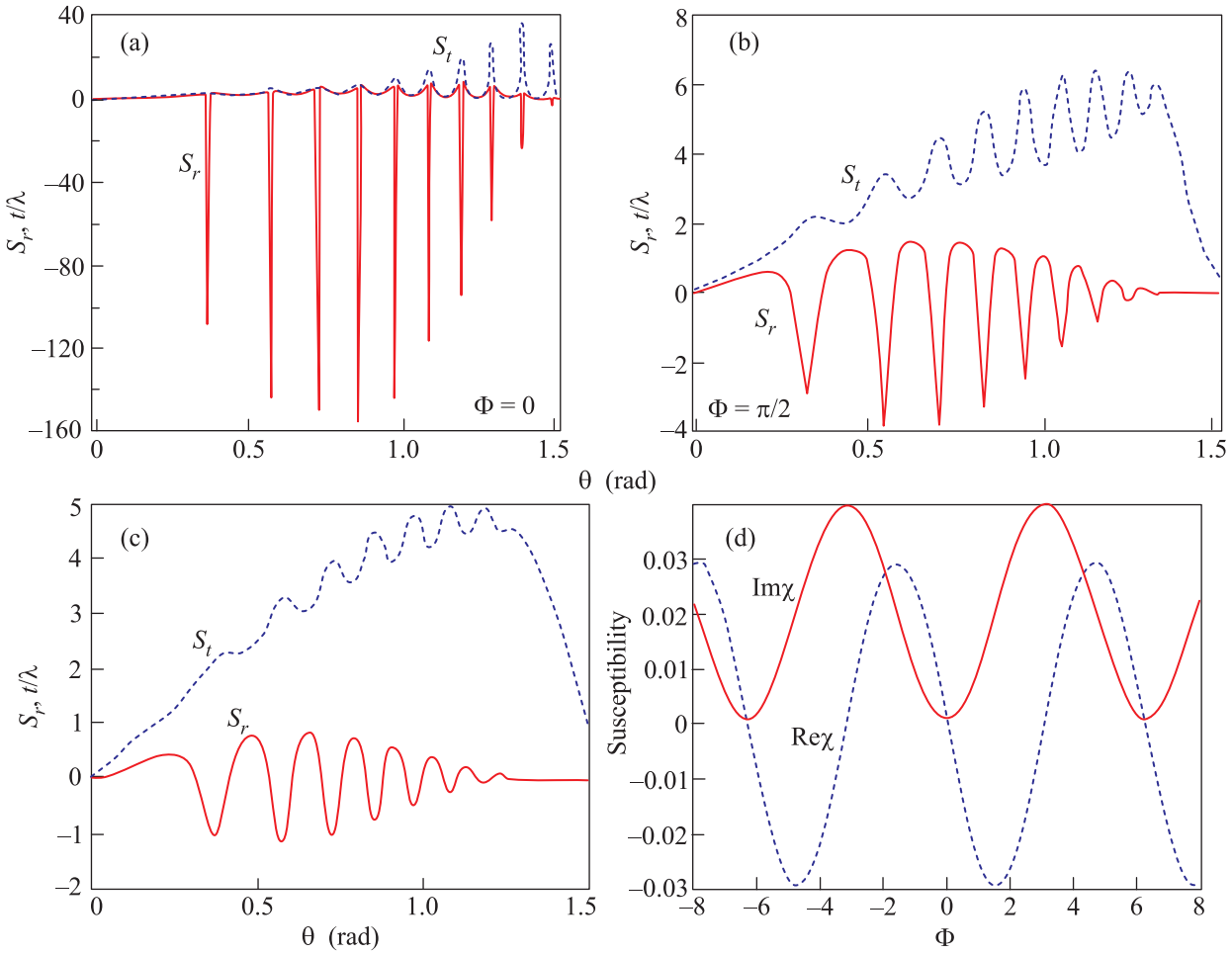

Fig. 2. The dependence of both S_r and S_t on the incident angel of probe light beam for $\Omega_{c1} = \Omega_{c2} = 5\gamma$, $\Omega_p = \Omega_s = 0.1\gamma$, $\gamma_a = \gamma_b = 0$, $\Delta_1 = \Delta_2 = \Delta_3 = 0$; $\phi = 0$ (a), $\pi/2$ (b), π (c), and the dependence of susceptibility versus relative phase of applied fields (d)

nonresonance and resonance conditions, the medium is transparent for the probe beams. However, the behaviors of GH shifts for reflected and transmitted beams are completely different when the relative phase changes from 0 to 2π. For $\phi = \pi/2$, the S_r and S_t can be enhanced and can be positive or negative at certain angles. Infact, for $\phi = \pi/2$, there is a net gain in the medium which makes the GH shifts of reflected and transmitted probe beams be positive or negative at certain angels. This tells us that the GH shift can be enhanced significantly by amplification at certain angels in the negative absorption region. It is known that the group index of the medium that is related to the superluminal and subluminal behavior of light propagation through the medium. The group index of the atomic medium can be calculated by using the real part of the susceptibility. In fact, for superluminal light propagation, the group index can be negative, while for subluminal light propagation it becomes positive. It should be noted that the behavior of the group index of the intracavity medium may be different from the behavior of the group index of the cavity. Therefore, we discuss the dependence of the GH shifts on the group index of the cavity corresponding to superluminal and subluminal light propagation. The group velocity of the reflected or transmitted light beam is given by:

$$v_g^{r,t} = \frac{L}{\tau_g^{r,t}}, \tag{16}$$

where $L = 2d_{\rm A} + d_{\rm B}$ is the total cavity thickness. The superscripts r, t correspond to the reflection and the transmission parts of the incident light probe beam. The corresponding group delay, i.e. $\tau_g^{r,t}$, is then given by:

$$\tau_g^{r,t} = \frac{\partial \phi_{r,t}}{\partial \omega} = \frac{\partial \phi_{r,t}}{\partial \omega_b}. \tag{17}$$

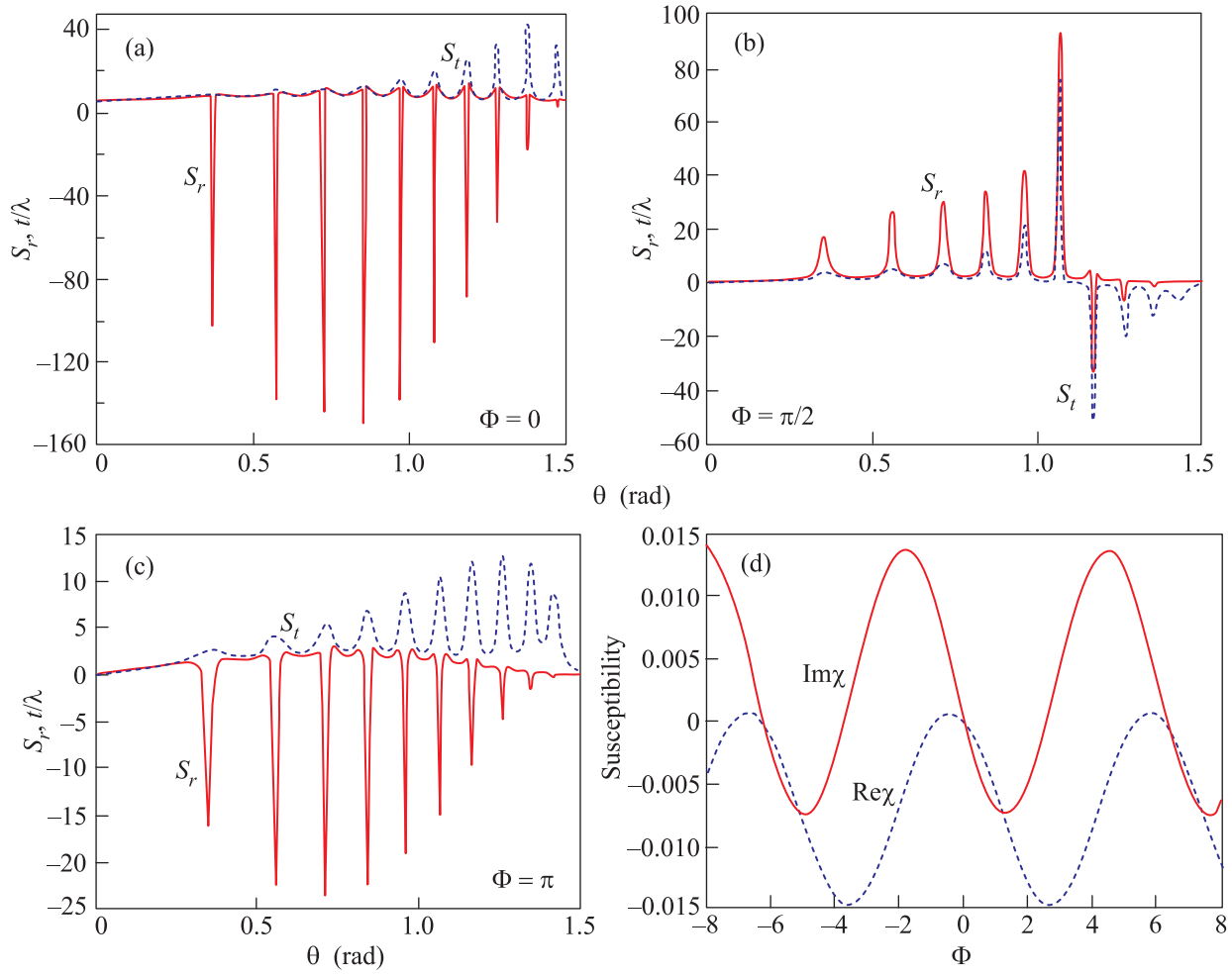

Fig. 3. The dependence of both S_r and S_t on the incident angel of probe light beam for $\Omega_{c1} = \Omega_{c2} = 5\gamma$, $\Omega_p = \Omega_s = 0.1\gamma$, $\gamma_a = \gamma_b = 0$, and $\Delta_1 = \Delta_2 = 2.5\gamma$, $\Delta_3 = 0$; $\phi = 0$ (a), $\pi/2$ (b), π (c), and the dependence of susceptibility versus relative phase of applied fields (d)

So, the cavity group index is defined as

$$n_g^{r,t} = \frac{c}{v_g^{r,t}} = \frac{c}{L}\frac{\partial \phi_{r,t}}{\partial \omega_b}. \qquad (18)$$

Relation (18) shows that the group index depends on the thickness of the cavity and the phase associated with the reflection and transmission coefficients. Therefore, the GH shifts depend on the sign of the group index $n_g^{r,t}$, that can be positive or negative depending on whether the group index is positive or negative, respectively. It is observed that the cavity group index for reflected and transmitted probe beams is positive (negative) whenever the GH shift is positive (negative). Therefore, by controlling the relative phase of applied fields the simultaneous positive or negative of group index for reflected and transmitted probe beams can be obtained. It can be seen that for $\phi = \pi/2$, the group index of reflected and transmitted probe beams both are positive or negative at certain angle. This is to say that the GH shifts for superluminal or subluminal case can be both negative and positive. In addition, the negative or positive GH shifts only occur for a certain choice of the incident angel. In this case, by controlling the angle of incident light one can control the GH shifts of superluminal or subluminal light propagation in the medium. The effect of relative phase on GH shifts of reflected and transmitted probe beams when we increase the Rabi frequencies of applied fields are shown in Fig. 4. It can be seen that for $\phi = 0.0$, the S_r and S_t is enhanced and can be positive or negative at certain angles, while for $\phi = \pi/2$, the peaks of GH shift in reflected (transmitted) beam suffer the negative (positive) shift. In this case, there is a weak absorption in the medium. But in Fig. 4c, the susceptibility of the medium becomes gain and both the S_r and S_t can be increased and are positive or negative at certain angels compared with in weak absorption region.

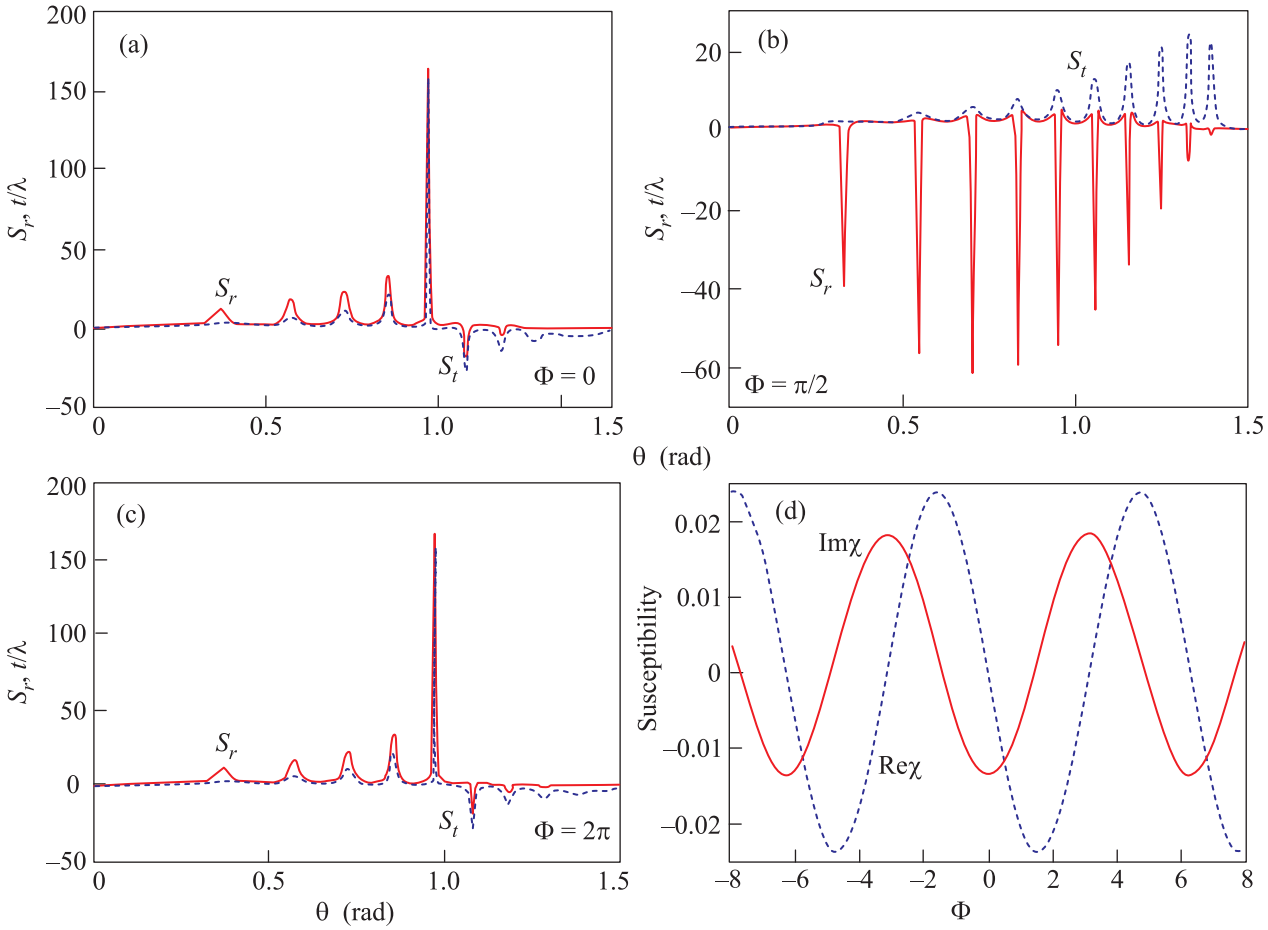

Fig. 4. The dependence of both S_r and S_t on the incident angel of probe light beam for $\Omega_{c1} = \Omega_{c2} = 10\gamma$, $\Omega_p = \Omega_s = 0.1\gamma$, $\gamma_a = \gamma_b = 0$, and $\Delta_1 = \Delta_2 = \Delta_3 = 0$; $\phi = 0$ (a), $\pi/2$ (b), 2π (c), and the dependence of susceptibility versus relative phase of applied fields (d)

These results tell us that the GH shift can be enhanced significantly by amplification in the negative absorption region. Our results show that the manipulation of the GH shifts of the reflected and transmitted probe beam can be easily controlled without changing the structure of the cavity and medium.

Conclusion. In summarize, the GH shifts of the reflected and transmitted probe beams in a four-level GaAs/AlGaAs quantum dot with 15 periods of 17.5 nm GaAs wells and 25-nm $Al_{0.3}Ga_{0.7}As$ barriers have been investigated. By controlling the external control parameters such as probe field detuning, relative phase of applied fields and Rabi frequencies of coupling field without changing the structure of the system. It is also shown that under the certain conditions, the large GH shifts of the reflected and transmitted probe beam can be both positive and negative in the gain region.

1. F. Goos and H. Hänchen, Ann. Phys. (Leipzig) **1**, 333 (1947).
2. J. Pichet, Ann. Phys. (Paris) **3**, 433 (1929).
3. T. Hashimoto and T. Yoshino, Opt. Lett. **14**, 913 (1989).
4. G. X. Li, J. Evers, and C. H. Keitel, Phys. Rev. B **80**, 045102 (2009).
5. X. Hu, Y. Huang, W. Zhang, D. K. Qing, and J. Peng, Opt. Lett **30**, 899 (2005).
6. G. Y. Oh, D. G. Kim, and Y. W. Choi, Opt. Express **17**, 20714 (2009).
7. M. Merano, A. Aiello, G. W. Hooft, M. P. Vanexter, E. R. Eliel, and J. P. Woerdman, Opt. Exp. **15**, 15928 (2007).
8. P. R. Berman, Phys. Rev. E **66**, 067603 (2002).
9. A. Lakhtakia, Electromanetics **23**, 71 (2003).
10. J. A. Kong, B. I. Wu, and Y. Zhang, Phys. Lett. A **80**, 2084 (2002).
11. X. Chen and C. F. Li, Phys. Rev. E **69**, 066617 (2004).
12. Y. Wu and X. Yang, Phys. Rev A **71**, 053806 (2005).
13. W. X. Yang, J. M. Hou, Y. Y. Lin, and R. K. Lee, Phys. Rev. A **79**, 033825 (2009).
14. L. G. Si, W. X. Yang, X. Y. Lou, X. Y. Hao, and X. Yang, Phys. Rev. A **82**, 013836 (2010).

15. J. H. Li, X. Y. Lou, J. M. Luo, and Q. J. Huang, Phys. Rev. A **74**, 035801 (2006).
16. S. H. Asadpour and A. Eslami-Majd, J. Lumin. **132**, 1477 (2012).
17. Z. Wang and B. Yu, Las. Phys. Lett. **11**, 035201 (2014).
18. D. Zhang, R. Yu, J. H. Li, X. Hao, and X. Yang, Opt. Comm. **321**, 138 (2014).
19. L. G. Si, W. X. Yang, and X. Yang, JOSA B **26**, 478 (2009).
20. Y. Wu and X. Yang, Phys. Rev. Lett. **98**, 013601 (2007).
21. Y. Wu and X Yang, Phys. Rev. A **70**, 053818 (2004).
22. L. G. Wang, M. Ikram, and M. S. Zubairy, Phys. Rev. A **77**, 023811 (2008).
23. Ziauddin, S. Qamar, and M. S. Zubairy, Phys. Rev. A **81**, 023821 (2010).
24. Ziauddin and S. Qamar, Phys. Rev. A **84**, 053844 (2011).
25. J. F. Dynes, M. D. Frogley, M. Beck, J. Faist, and C. C. Philips, Phys. Rev. Lett. **94**, 157403 (2005).
26. J. H. Li, Phys. Rev. B **75**, 155329 (2007).
27. J. H. Li and X. X. Yang, Eur. Phys. J. B **53**, 449 (2006).
28. A. Joshi and M. Xiao, Appl. Phys. B **79**, 65 (2004).
29. Z. Wang and B. Yu, J. Appl. Phys. **113**, 113101 (2013).
30. S. H. Asadpour, M. Jaberi, and H. R. Soleimani, JOSA B, 2223 (2014).
31. W. X. Yang, J. M. Hou, and R. K. Lee, Phys. Rev. A **77**, 033838 (2008).
32. W. X. Yang, A. X. Chen, L. G. Si, K. Jiang, X. Yang, and R. K. Lee, Phys. Rev. A **81**, 023814 (2010).
33. X. X. Yang, Z. W. Li, and Y. Wu, Phys. Lett. A **340**, 320 (2005).
34. S. H. Asadpour, M. Sahrai, R. Sadighi-Bonabi, A. Soltani, and H. Mahrami, Physica E **43**, 1759 (2011).
35. S. H. Asadpour, H. R. Hamedi, A. Eslami-Majd, and M. Sahrai, Physica E **44**, 464 (2011).
36. M. Phillips and H. L. Wang, Phys. Rev. Lett. **89**, 186401 (2002).
37. M. C. Phillips and H. L. Wang, Phys. Rev. Lett. **91**, 183602 (2003).
38. M. C. Phillips and H. L. Wang, Phys. Rev. B **69**, 115337 (2004).
39. G. B. Serapiglia, E. Paspalakis, C. Sirtori, K. L. Vodopyanov, and C. C. Philips, Phys. Rev. Lett. **84**, 1019 (2000). 13
40. J. F. Dynes, M. D. Forgley, J. Rodger, and C. C. Philips, Phys. Rev. B: Cond. Mat. **72**, 085323 (2005).
41. J. F. Dynes, M. D. Forgley, M. Beck, J. Faist, and C. C. Philips, Phys. Rev. Lett. **94**, 157404 (2005).
42. S. G. Carter, V. Birkedal, and C. S. Wang, Science **310**, 651 (2005).
43. M. Philips and H. Wang, Opt. Lett. **28**, 831 (2003).
44. M. Lindberg and R. Binder, Phys. Rev. Lett. **75**, 1403 (1995).
45. S. Marcinkevicius, A. Gushterov, and J. P. Reithmaier, Appl. Phys. Lett. **92**, 041113 (2008).
46. C. J. Chang-Hasnain, P. C. Ku, J. Kim, and S. L. Chuang, Proc. IEEE **91**, 1884 (2003).
47. W. W. Chow, H. C. Schneider, and M. C. Philips, Phys. Rev. A: At. Mol. Opt. Phys. **68**, 053802 (2003).
48. T. R. Nielsen, A. Lavrinenko, and J. Mork, Appl. Phys. Lett. **94**, 113111 (2009).
49. A. A. Belyanin, F. Capasso, V. V. Kocharovsky, VI.V. Kocharovsky, and M. O. Scully, Phys. Rev. A **63**, 053 803 (2001).
50. I. V. Soboleva, V. V. Moskalenko, and A. A. Fedyanin, Phys. Rev. Lett. **108**, 123901 (2012).
51. S. H. Asadpour and H. R. Soleimani, Opt. Commun. **315**, 347 (2014).
52. S. H. Asadpour and H. R. Soleimani, Physica B **440**, 124 (2014).
53. W. X. Yang, A. X. Chen, R. K. Lee, and Y. Wu, Phys. Rev. A **84**, 013835 (2011).
54. C. Ding, X. Hao, J. Li, and X. Yang, Phys. Lett. A **374**, 680 (2010).